

Supplemental Information for V. Chan *et al.* (2015)

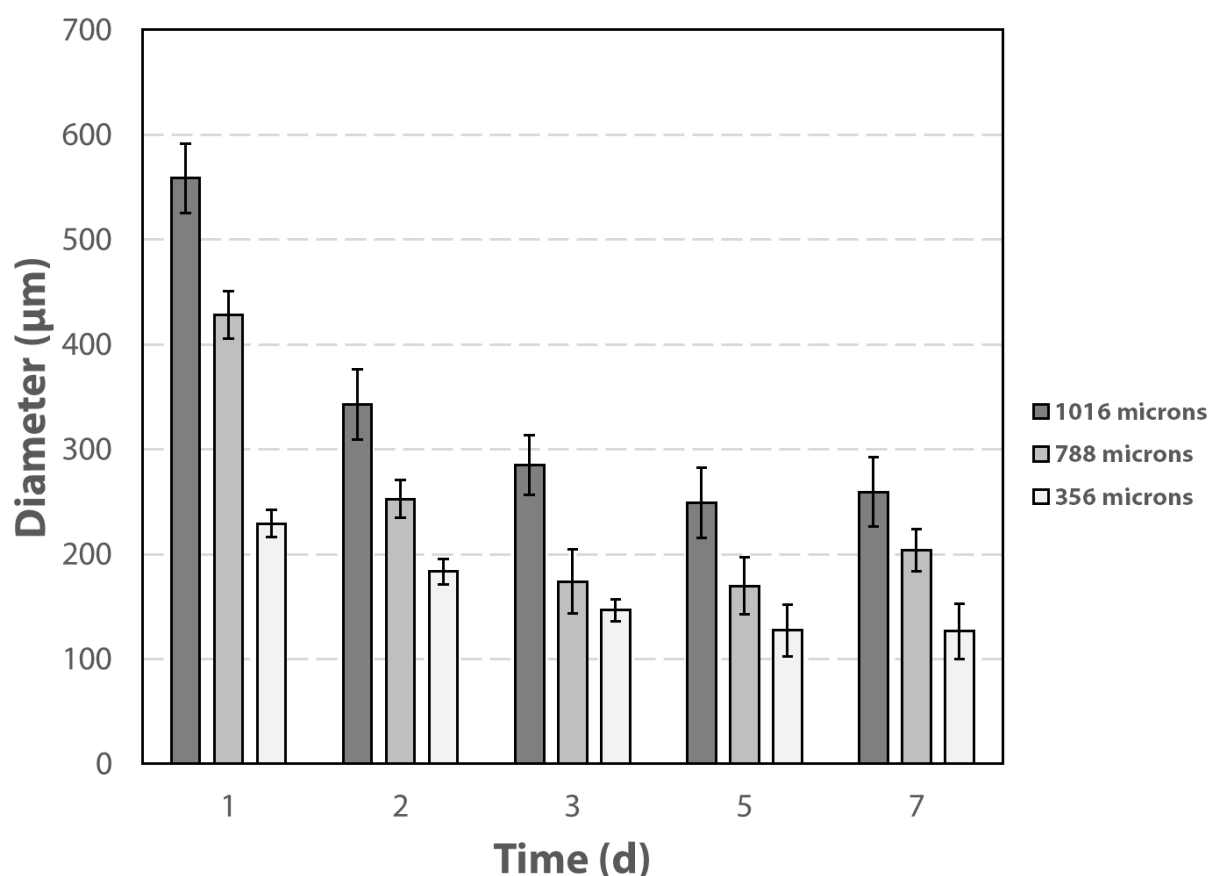


Figure S1. Cell-mediated compaction of cardiac muscle strips over time using various removal pin diameters. Cardiac muscle strips made with various removable pin diameters (356, 788, and 1016 μm) were produced and changes in construct diameters were monitored using phase contrast images over the course of a week. We measured the diameter at each point along the length and at each time point by using a custom MATLAB code. This graph shows changes in the average diameter computed for the entire length of each construct over time.

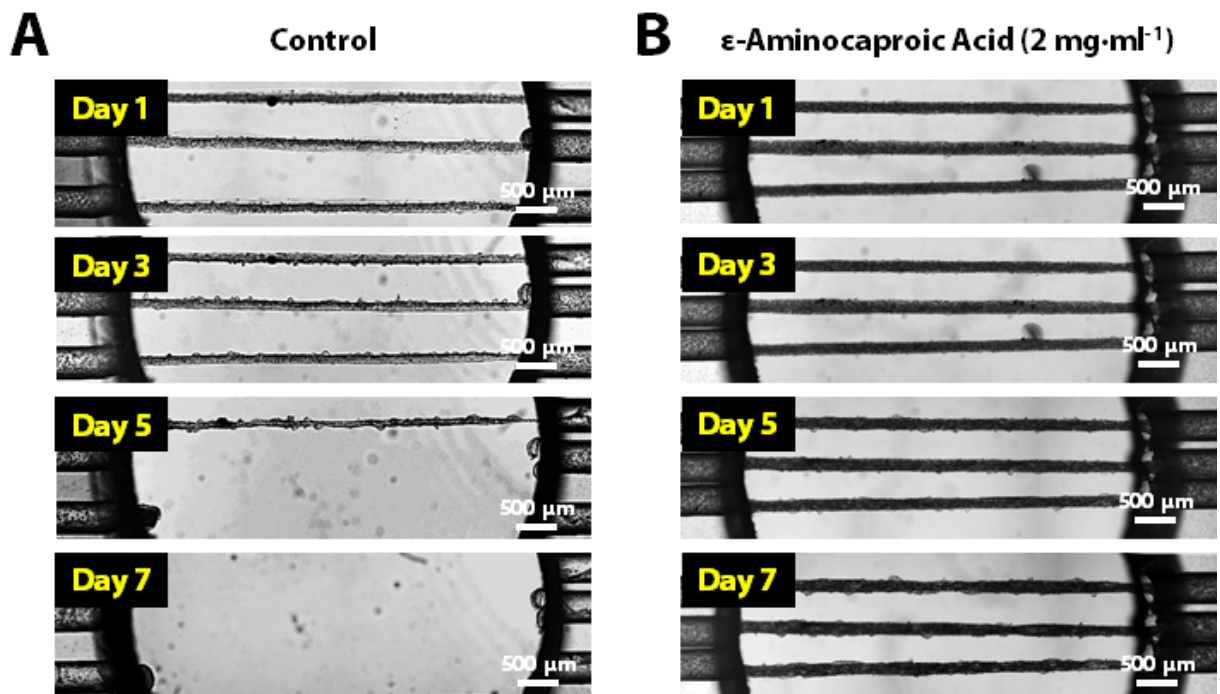


Figure S2. Prevention of cardiac muscle strip degradation over time with ε-aminocaproic acid (EACA). (A) In the preparation of cell culture medium for the entrapment of primary cardiac myocytes with fibrin, the cardiac muscle strips exhibited non-uniform diameter and degraded completely within a week. (B) EACA at 2 mg·ml⁻¹ concentration was used to inhibit fibrin degradation by the cells.

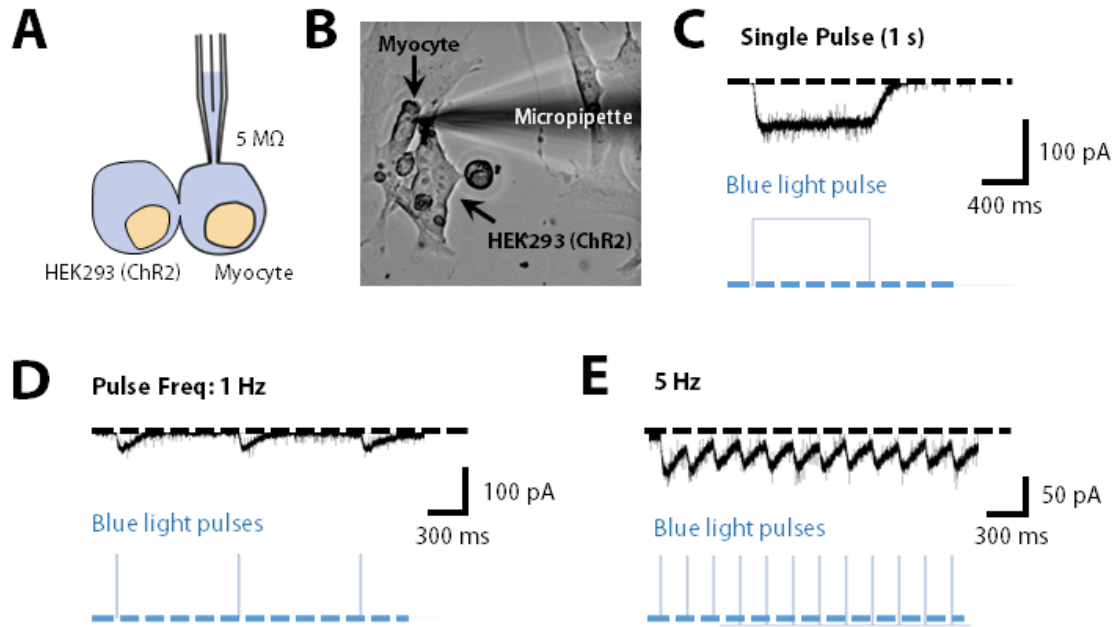


Figure S3. Electrophysiology of HEK293T cells expressing channelrhodopsin-2 joined to primary cardiac myocytes. (A) Patch clamp recordings were performed on 2D co-cultures of HEK293T (ChR2) and cardiac myocytes within 48 hr after isolation. (B) A brightfield microscopy image of joint myocyte-HEK293 (ChR2) cells with micropipette sealed over the membrane of the myocyte. (C) A single pulse of blue light (1 second) resulted in the depolarization of the patched HEK-ChR2 cell and propagation to the myocyte. The same cells were also stimulated at (D) 1 and (E) 5 Hz with visible depolarization of myocytes.

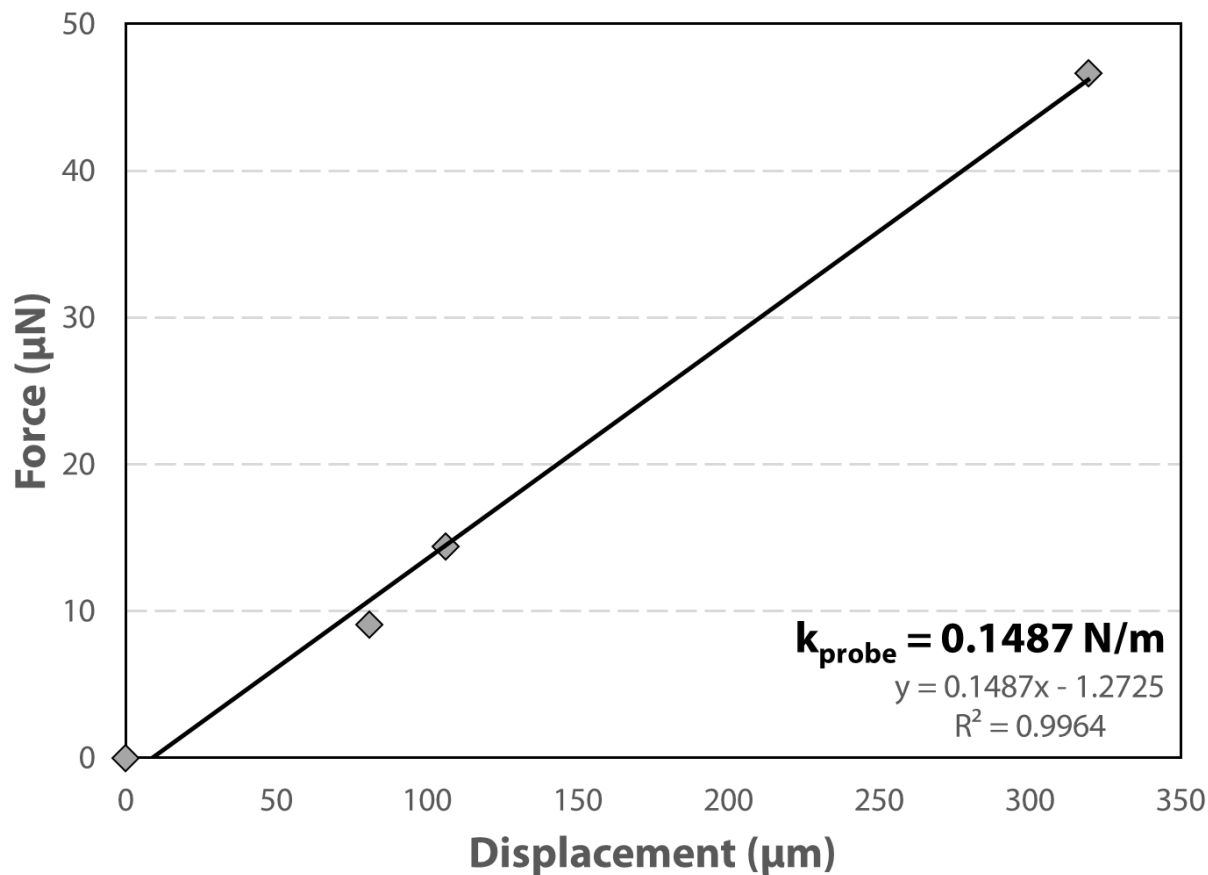


Figure S4. Force-displacement curve for 40 gauge (G) copper wire calibration to estimate probe tip stiffness. The copper probe was calibrated by hanging known wire weights against gravity on the probe tip. The probe was mounted horizontally on the microscope stage, and tweezers were used to position the wire weights on the end of the probe tip. The optical axis of the microscope was used to measure the difference in focal planes between the loaded and unloaded tip to determine the amount of probe bending. The measurements were used to generate a load vs. displacement curve, which was then fit using linear regression to determine estimated cantilever stiffness ($k_{\text{probe}} = 0.1487 \text{ N/m}$).

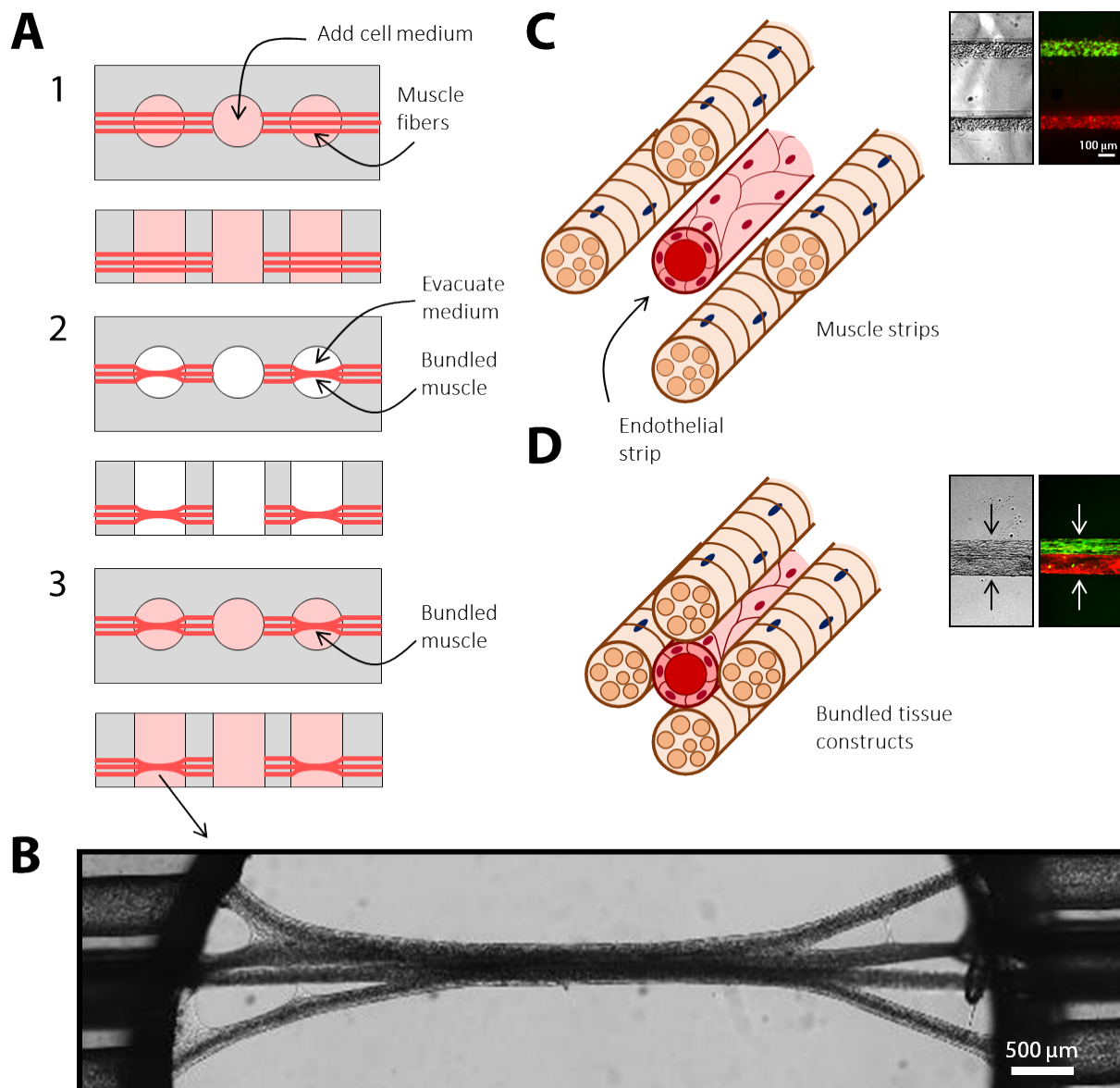


Figure S5. Bundled muscle tissue strips for greater hierarchical constructs with multiple cell types. (A) Schematic overhead and cross-sectional view of multi-strip bundling method. Bundling was achieved by removing most or all of the culture medium in the well to generate surface tension between the tissues to permit physical contact. (B) Brightfield microscopy of a multi-strip bundle by stitching several acquired images together. (C) The multi-strip technique can be used to culture multiple cell types separately, such as muscle and endothelial cells, to form mature tissues with appropriate structure. Inset: Brightfield and fluorescence microscopy of two strips with different populations of cells. (D) Once mature, these multi-strips can be bundled into a single construct with multiple cell types. Inset: Brightfield and fluorescence microscopy of bundled construct with two different populations of cells.

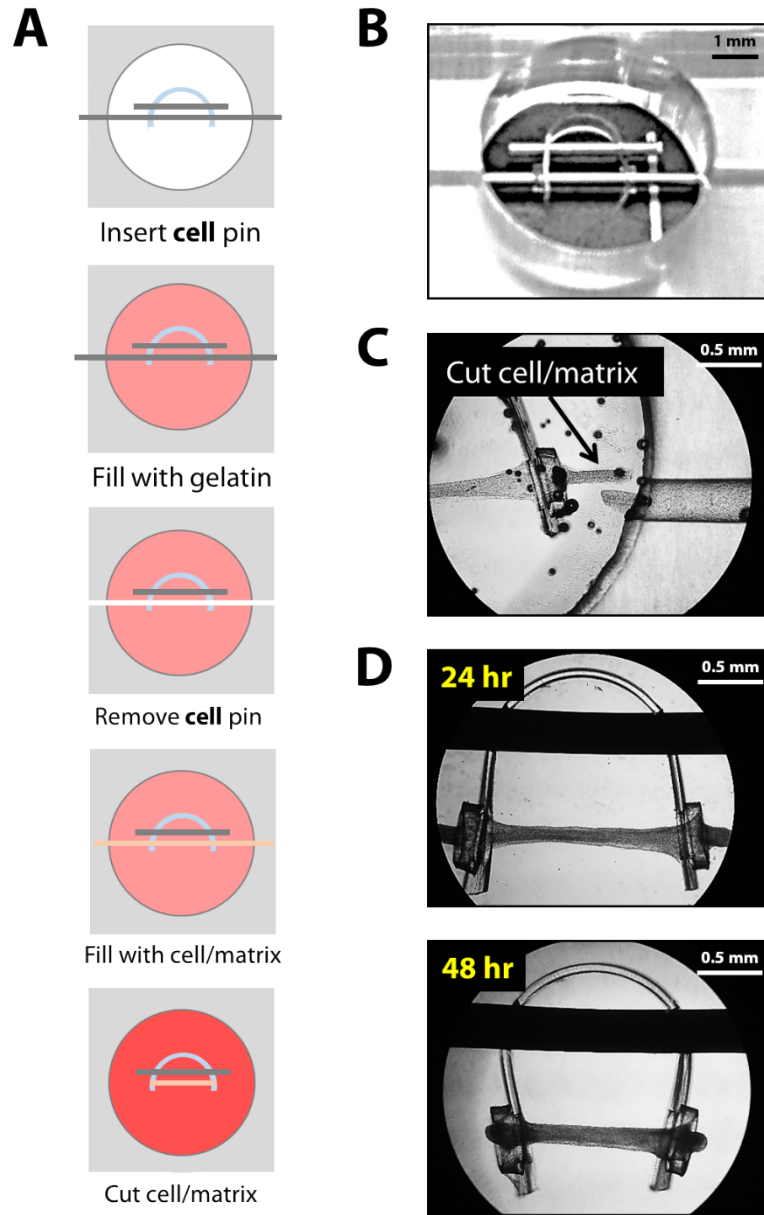


Figure S6. Fabrication and formation of a muscle strip in a free-floating device for bio-actuation. (A) Schematic fabrication process of free-floating devices with muscle strips. Devices were built by spin-coating PDMS material on a glass slide to a pre-determined thickness. (B) After curing, the PDMS was cut into C-shapes that were held in place by a short steel pin and loaded into wells using another steel pin that traversed the through holes in the well. The sacrificial outer molding technique was then carried out as described in the *Materials and Methods* to form muscle strips. (C) C-shaped devices were detached from the wells by cutting the muscle strips at the ends. (D) After 48 hr, the muscle strips compacted to its final form. Similar devices can be constructed for bio-robotic applications, such as bio-actuation with increased force and control.

Movie Legends for V. Chan *et al.* (2015)

Movie S1. A 30 s video clip of a cardiac muscle strip segment 48 hr post-formation (bottom view). Cells were predominantly spherical, although a small number began to elongate along the longitudinal axis. Spontaneous contractions of single cells were sporadic with regional areas of synchronous contractions beginning to emerge.

Movie S2. A 30 s video clip of a cardiac muscle strip segment 72 hr post-formation (bottom view). At this time point, the majority of cells had elongated along the longitudinal axis with many creating specialized intercellular connections. Spontaneous contractions are mainly regional with few sporadic single cell contractions.

Movie S3. A 30 s video clip of a cardiac muscle strip segment 120 hr post-formation (bottom view). The muscle strip had fully compacted, and most of the cells were aligned along the longitudinal axis. The cells were connected in one large 3D syncytium, which is synchronized electrically in an action potential.

Movie S4. A 60 s video clip demonstrating light-activated spatial recruitment of three horizontally-aligned cardiac muscle strips (bottom view). Eight different combinations can be generated with four of them shown here: (1) bottom strip, (2) middle strip, (3) bottom and middle strips, and (4) all three strips. Selective recruitment was achieved by adjusting the size and position of light exposure.

Movie S5. A 60 s video clip illustrating force characterization of three vertically-aligned cardiac muscle strips (bottom view). The muscle strips were laterally stretched with a copper probe to various distances to apply tension and illuminated with blue light to stimulate contraction. The displacements of the copper probe were then tracked and recorded.

Movie S6. An animated movie of the applied tension and illuminated contraction. This movie is to supplement for Movie S5 for clarity purposes.